RESEARCH ARTICLE

Figures and figure supplements

Evolutionary rescue of phosphomannomutase deficiency in yeast models of human disease

Ryan C Vignogna *et al*

A

Human Variant	Yeast Equivalent	Effect	Relative Enzyme Activity	Relative Growth Rate p*SEC53* (1x)	Relative Growth Rate p*ACT1* (2x)
PMM2	*SEC53*	Wild-type	1.00	1.00	1.00
pmm2-V231M	*sec53*-V238M	Decreased Stability	0.39	0.32	0.67
pmm2-F119L	*sec53*-F126L	Reduced Dimerization	0.25	0.27	0.57

B

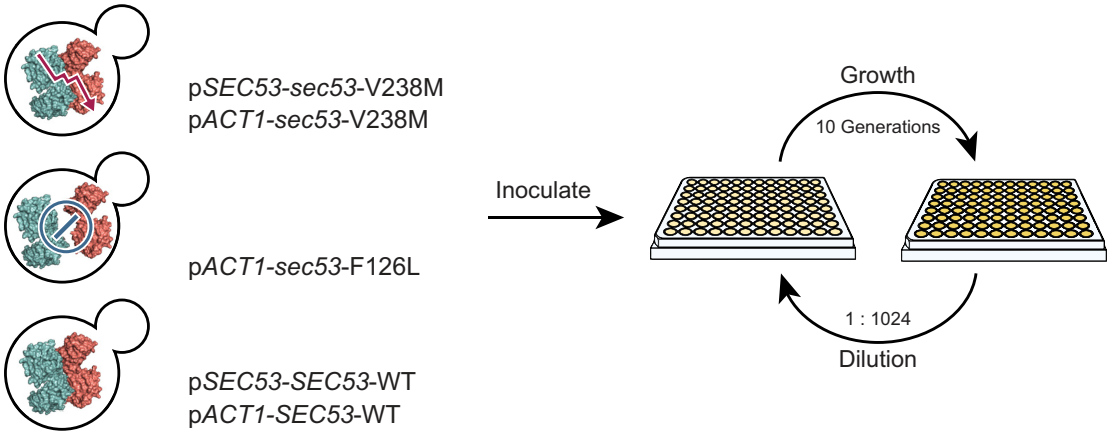

C

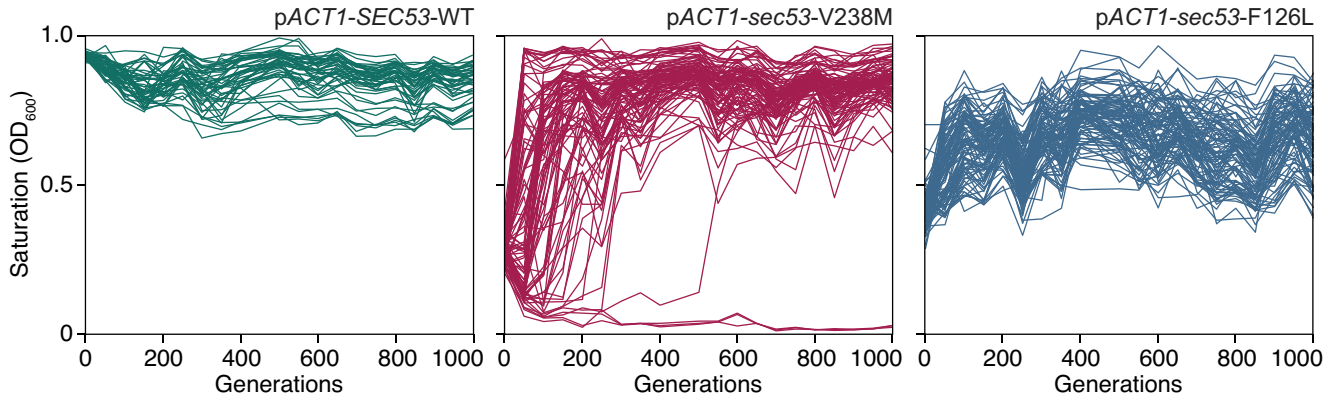

Figure 1. Experimental evolution of yeast models of congenital disorders of glycosylation. (**A**) Table of the various *sec53* alleles used in this study. In vitro enzymatic activities of Pmm2 are relative to wild-type Pmm2 and were previously reported (***Pirard et al., 1999***). Relative growth rates of yeast carrying various *SEC53* alleles were previously reported (***Lao et al., 2019***). (**B**) Diagram of the evolution experiment. Yeast carrying *sec53* mutations implicated in human disease were used to initiate replicate populations in 96-well plates: 96 populations of each mutant genotype and 48 populations of each wild-type genotype. Populations were propagated in rich glucose media, unshaken, for 1000 generations. (**C**) Single time-point OD_{600} readings of populations were taken every 50 generations during the evolution experiment as a measure of growth rate. Each line represents one population.

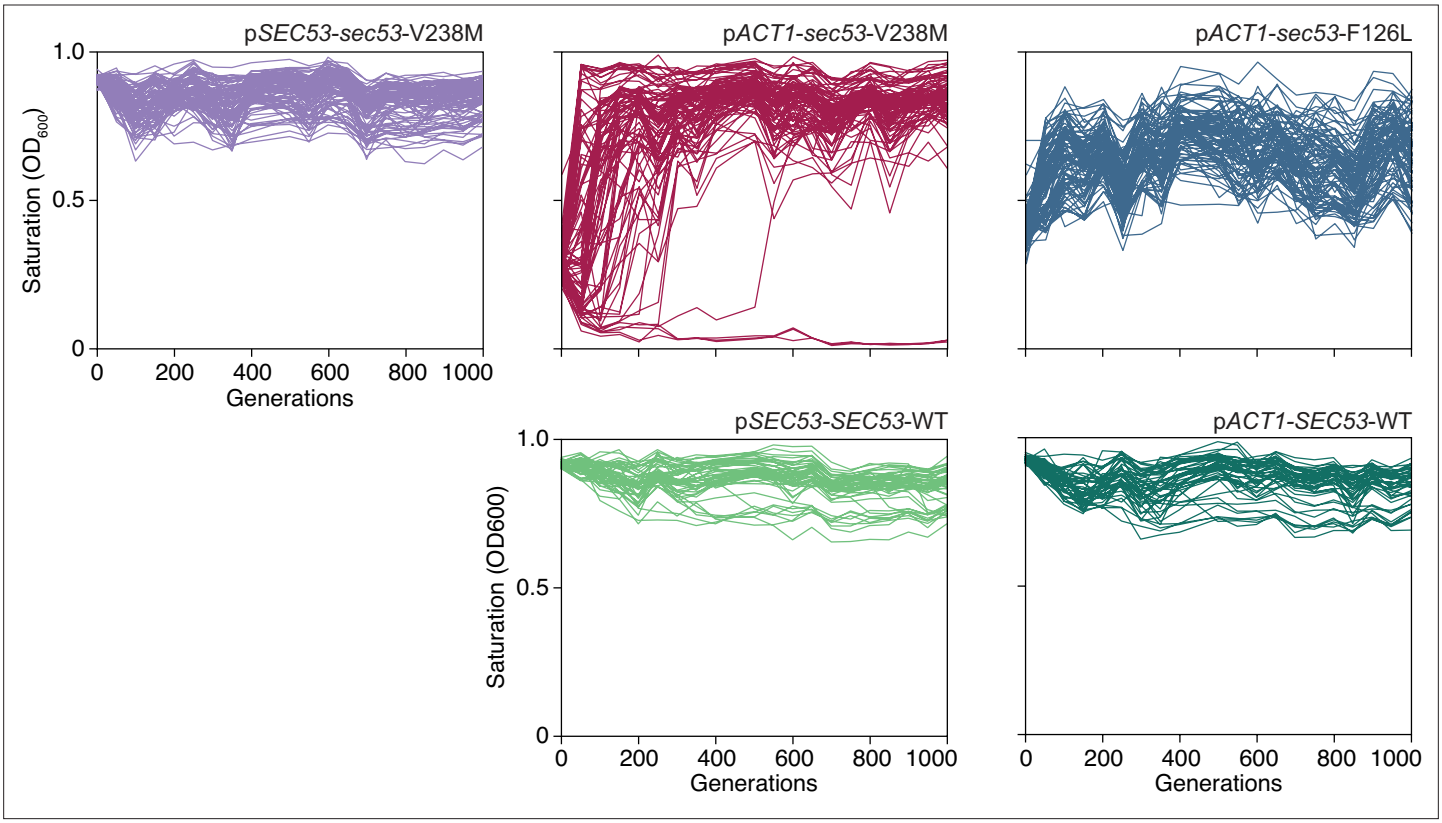

Figure 1—figure supplement 1. OD_{600} readings of each population. Single time-point OD_{600} readings of populations over the course of the evolution experiment. Every 50 generations, following daily transfer, populations were resuspended and OD was measured. Each line represents one population.

A

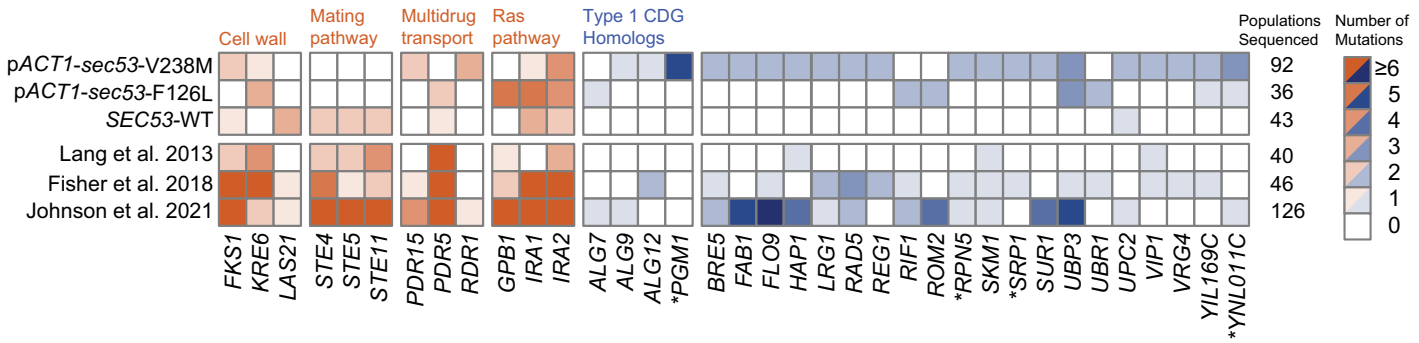

B

	p*ACT1-sec53*-V238M	p*ACT1-sec53*-F126L	*SEC53*-WT	Combined WT
Nuclear genes	5,906	5,906	5,906	5,906
Nonsynonymous mutations	297	178	146	9,933
Type 1 CDG genes	24	24	24	24
Type 1 CDG nonsynonymous mutations	7	1	0	20
Expected	1.2	0.7	0.6	40.4
Binomial Enrichment p-value	***0.00025***	0.52	1	0.99986
Binomial Depletion p-value	0.99996	0.84	0.55	***0.00030***

Figure 2. Mutations in Type 1 congenital disorders of glycosylation (CDG) homologs are enriched in *sec53*-V238M populations. (**A**) Heatmap showing the number of nonsynonymous mutations per gene that arose in the evolution experiment. Genes with two or more unique nonsynonymous mutations (and each Type 1 CDG homolog with at least one mutation) are shown. p*SEC53-SEC53*-WT and p*ACT1-SEC53*-WT are grouped as '*SEC53*-WT'. For comparison, we show data from previously reported evolution experiments where the experimental conditions were identical to the conditions used here, aside from strain background and experiment duration (bottom three rows). Commonly mutated pathways are grouped for clarity. Asterisks (*) indicate previously known *SEC53* genetic interactors (***Costanzo et al., 2016***; ***Kuzmin et al., 2018***). (**B**) Binomial test for enrichment or depletion of mutations in Type 1 CDG homologs based on the number of nonsynonymous mutations observed in each experiment, the total number of yeast genes (5906), and the number of genes that are Type 1 CDG homologs (24). 'Combined WT' includes the *SEC53*-WT populations as well as three additional datasets: ***Lang et al., 2013***, ***Fisher et al., 2018***, and ***Johnson et al., 2021***.

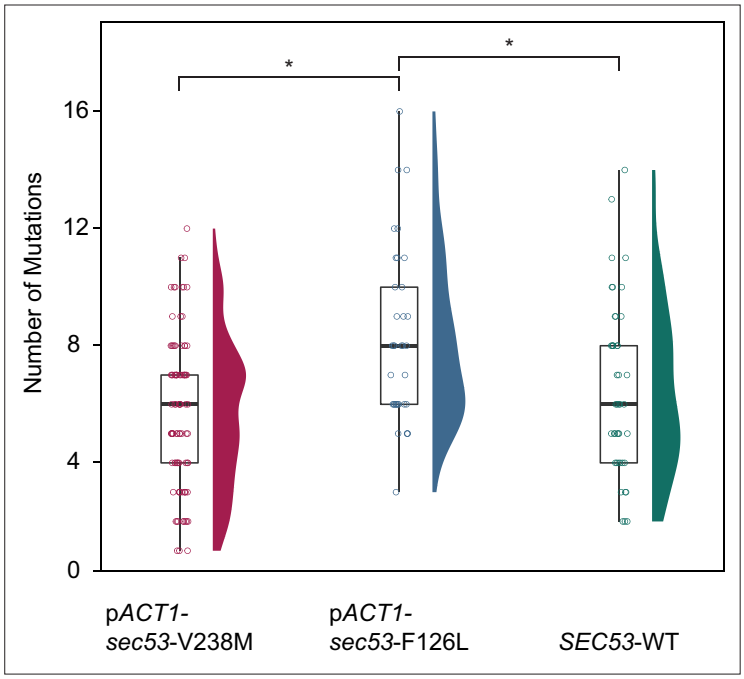

Figure 2—figure supplement 1. The number of de novo mutations per *SEC53* genotype. Each circle represents the number of SNPs and small indels present in a sequenced clone (***Supplementary file 1***). p*SEC53-SEC53*-WT and p*ACT1-SEC53*-WT are grouped as '*SEC53*-WT'. Distribution of points are shown as violin plots. Only statistically significant differences shown ($p < 0.05$) with bars and astersisks (*). p*ACT1-sec53*-V238M versus *SEC53*-WT ($p = 0.326$), p*ACT1-sec53*-V238M versus p*ACT1-sec53*-F126L ($p > 0.0001$), p*ACT1-sec53*-F126L versus *SEC53*-WT ($p = 0.0234$) (df = 167, $F = 9.67$, one-way analysis of variance [ANOVA] with Tukey post hoc test).

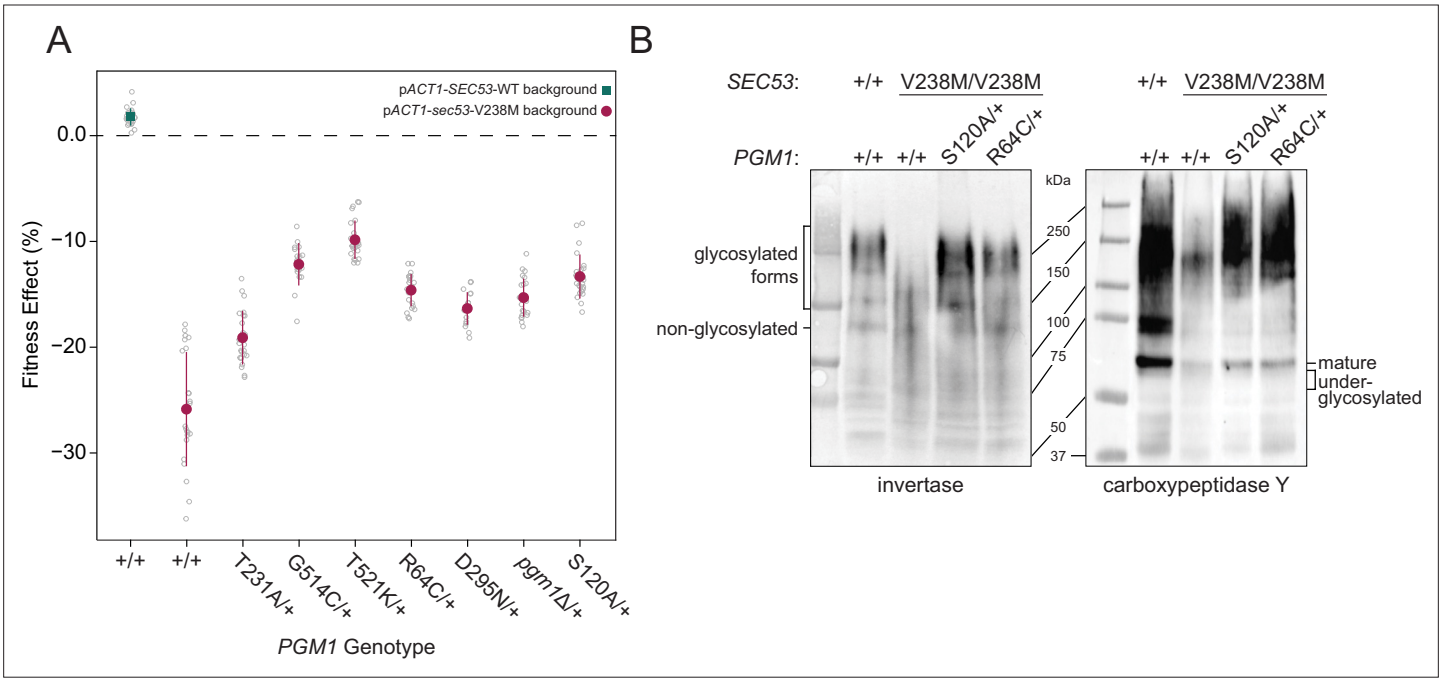

Figure 3. Evolved mutations rescue fitness and protein glycosylation defects of p*ACT1-sec53*-V238M. (**A**) Average fitness effects and standard deviations of reconstructed heterozygous *pgm1* mutations. Fitness effects were determined by competitive fitness assays against a fluorescently labeled version of the diploid p*ACT1-SEC53*-WT ancestor. Replicate measurements are plotted as gray circles. Pairs of *pgm1* fitness effects with non-statistically significant differences: R64C-D295N, R64C-*pgm1*Δ, R64C-S120A, D295N-*pgm1*Δ, G514C-T521K, G514C-S120A, and *pgm1*Δ-S120A (df = 194, $F = 208.1$, each $p > 0.05$, one-way analysis of variance [ANOVA] with Tukey post hoc test). (**B**) Western blots of invertase (left) and carboxypeptidase Y (right) from ancestral and reconstructed strains. In panels A and B, plus signs (+) indicate wild-type alleles. Genotypes are either homozygous wild-type (+/+), homozygous mutant (mutation/mutation), or heterozygous (mutation/+).

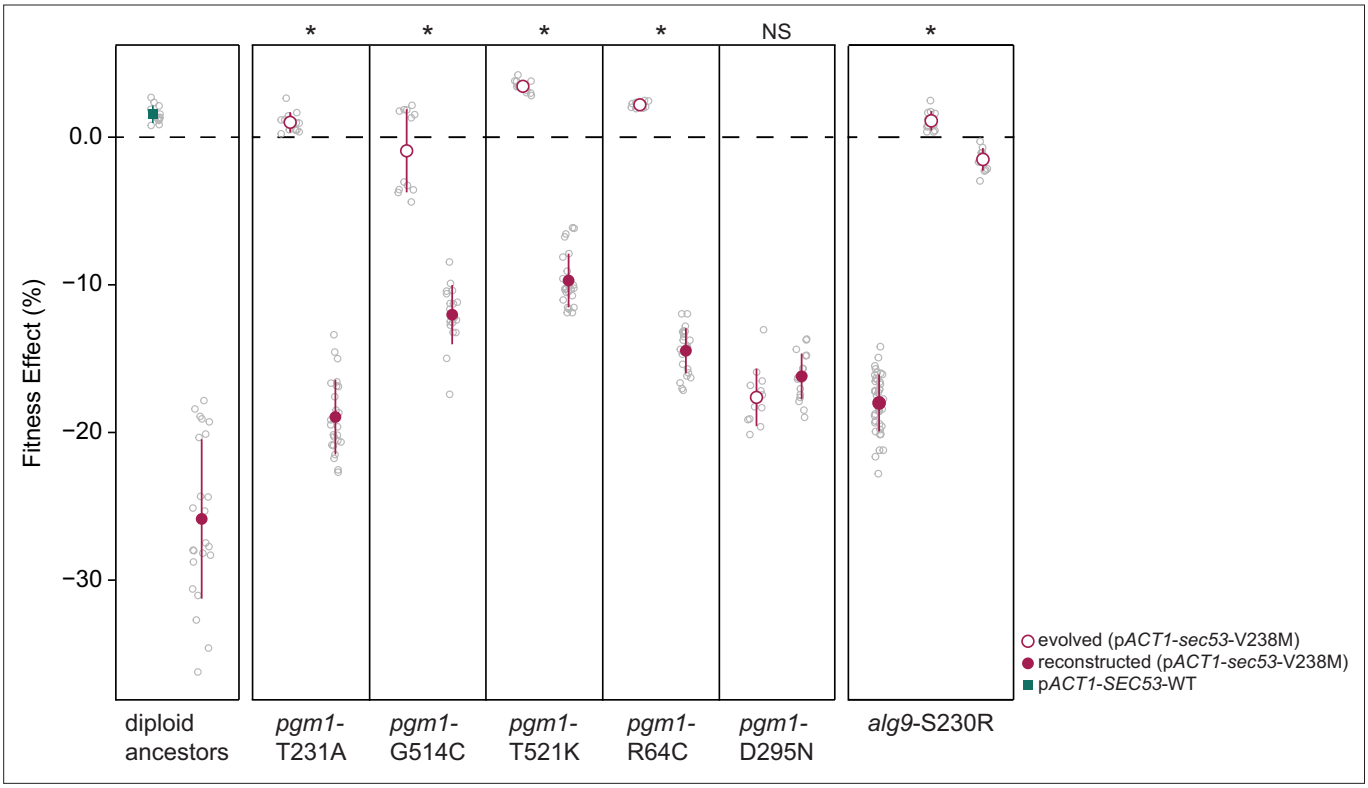

Figure 3—figure supplement 1. Fitness effects of reconstructed mutations and evolved clones containing those same mutations. Average fitness effects and standard deviations of reconstructed heterozygous *pgm1* and *alg9* mutations (closed circles) compared to evolved clones containing those mutations plus three to nine additional mutations (open circles). Replicate measurements are plotted as gray circles. Note there are two clones from different populations with an *alg9*-S230R mutation. Asterisks (*) represent statically significant differences between fitness effects of evolved clones and fitness effects of reconstructed clones (Welch's modified *t*-test): *pgm1*-T231A ($p < 0.0001$, $t = 36.1$, df = 28.9); *pgm1*-G514C ($p < 0.0001$, $t = 11.8$, df = 18.4); *pgm1*-T521K ($p < 0.0001$, $t = 33.8$, df = 27.3); *pgm1*-R64C ($p < 0.0001$, $t = 52.9$, df = 24.3); *pgm1*-D295N ($p = 0.05$, $t = 2.10$, df = 19.9); *alg9*-S230R (left) ($p < 0.0001$, $t = 53.7$, df = 49.7); *alg9*-S230R (right) ($p < 0.0001$, $t = 44.1$, df = 46.1).

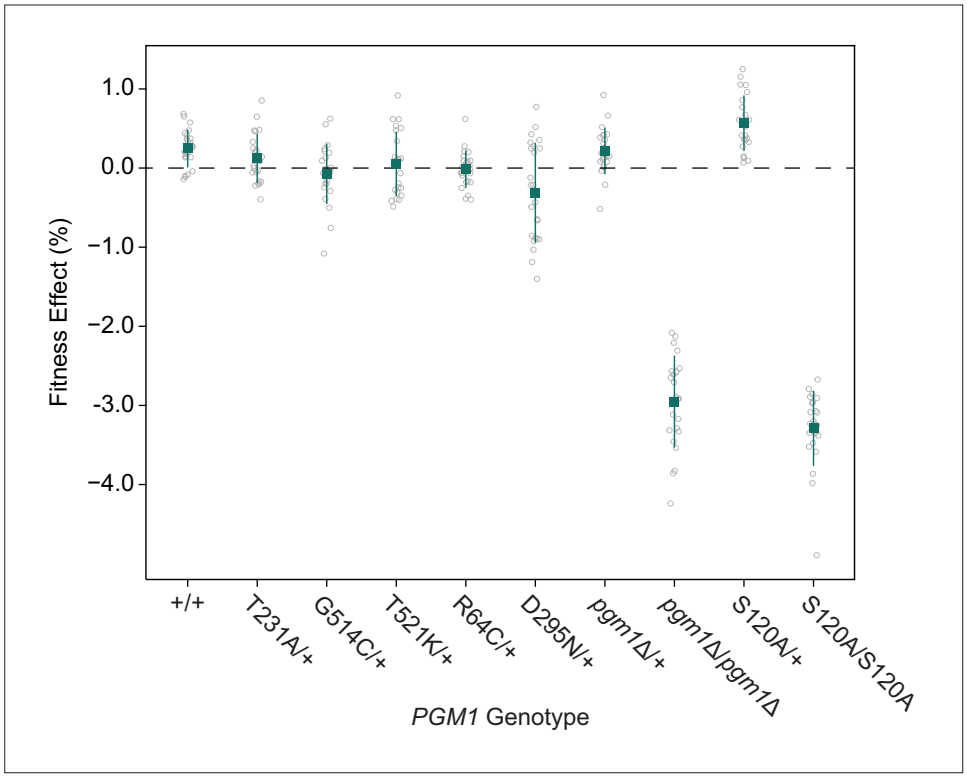

Figure 3—figure supplement 2. Fitness effects of *pgm1* mutations in the *SEC53*-WT background. Average fitness effects and standard deviations of reconstructed *pgm1* mutations in the diploid p*ACT1-SEC53*-WT background. Replicate measurements are plotted as gray circles. Plus signs (+) indicate wild-type alleles.

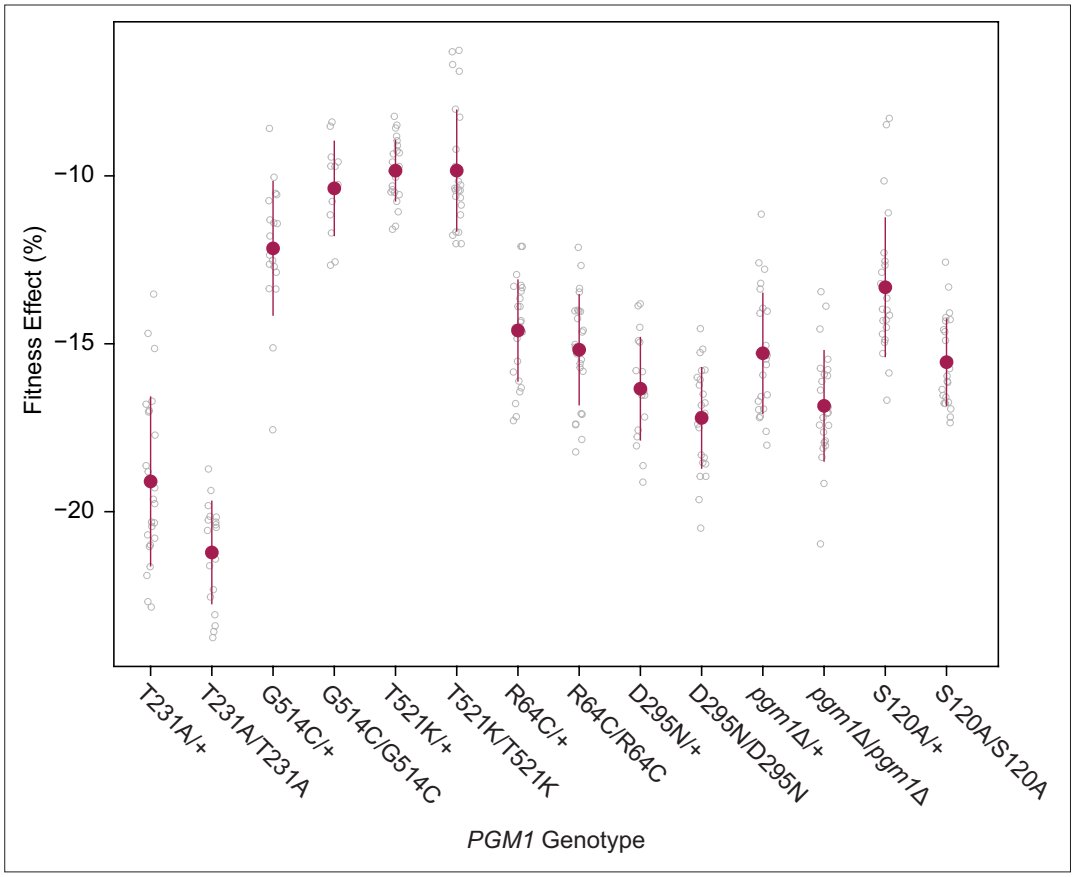

Figure 3—figure supplement 3. Fitness effects of homozygous *pgm1* mutations. Average fitness effects and standard deviations of reconstructed *pgm1* mutations in the diploid p*ACT1-sec53*-V238M background as heterozygous (mutation/+) or homozygous (mutation/mutation) alleles. Replicate measurements are plotted as gray circles. Comparison of heterozygous and homozygous allele fitness effects (Welch's modified *t*-test): *pgm1*-T231A ($p = 0.002$, $t = 3.35$, $df = 38.6$); *pgm1*-G514C ($p = 0.008$, $t = 2.85$, $df = 27.8$); *pgm1*-T521K ($p = 0.996$, $t = 0.005$, $df = 34.0$); *pgm1*-R64C ($p = 0.219$, $t = 1.24$, $df = 45.7$); *pgm1*-T231A ($p = 0.077$, $t = 1.84$, $df = 36.4$); *pgm1*Δ ($p = 0.003$, $t = 3.12$, $df = 45.7$); *pgm1*-S120A ($p < 0.0001$, $t = 4.45$, $df = 38.6$).

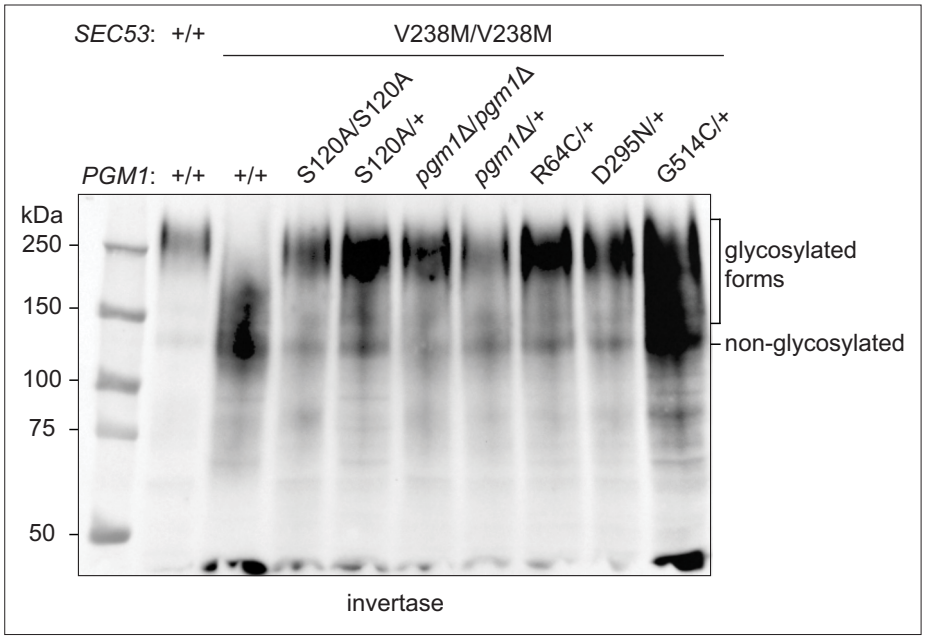

Figure 3—figure supplement 4. Effects of *pgm1* mutations on invertase glycosylation in the p*ACT1-sec53*-V238M background. Western blot of invertase from reconstructed *sec53*/*pgm1* strains.

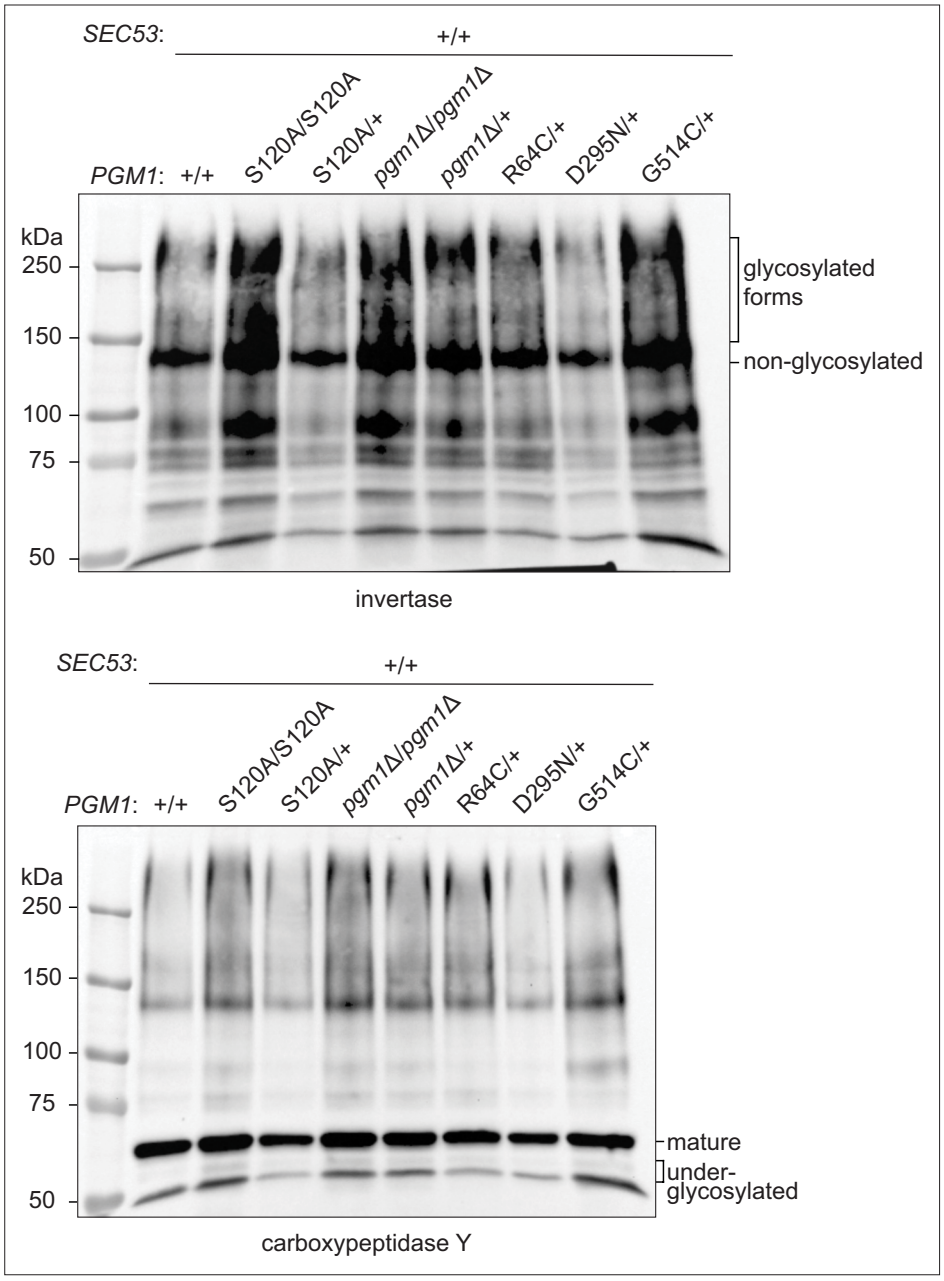

Figure 3—figure supplement 5. Effects of *pgm1* mutations on invertase and carboxypeptidase Y (CPY) glycosylation in the p*ACT1-SEC53*-WT background. Western blots of invertase and CPY from constructed *SEC53*/*pgm1* strains.

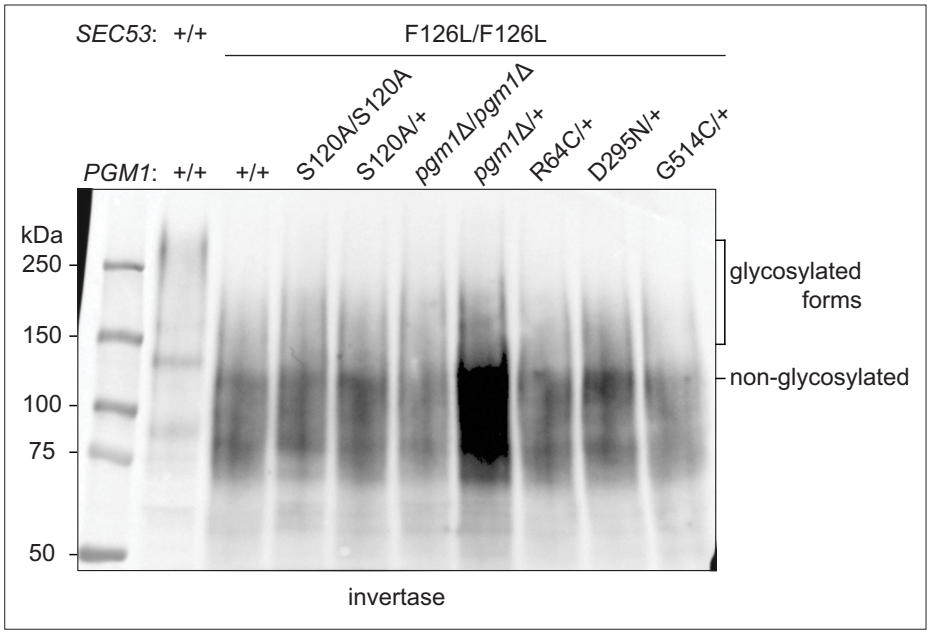

Figure 3—figure supplement 6. Effects of *pgm1* mutations on invertase glycosylation in the p*ACT1-sec53*-F126L background. Western blot of invertase from reconstructed *sec53*/*pgm1* strains.

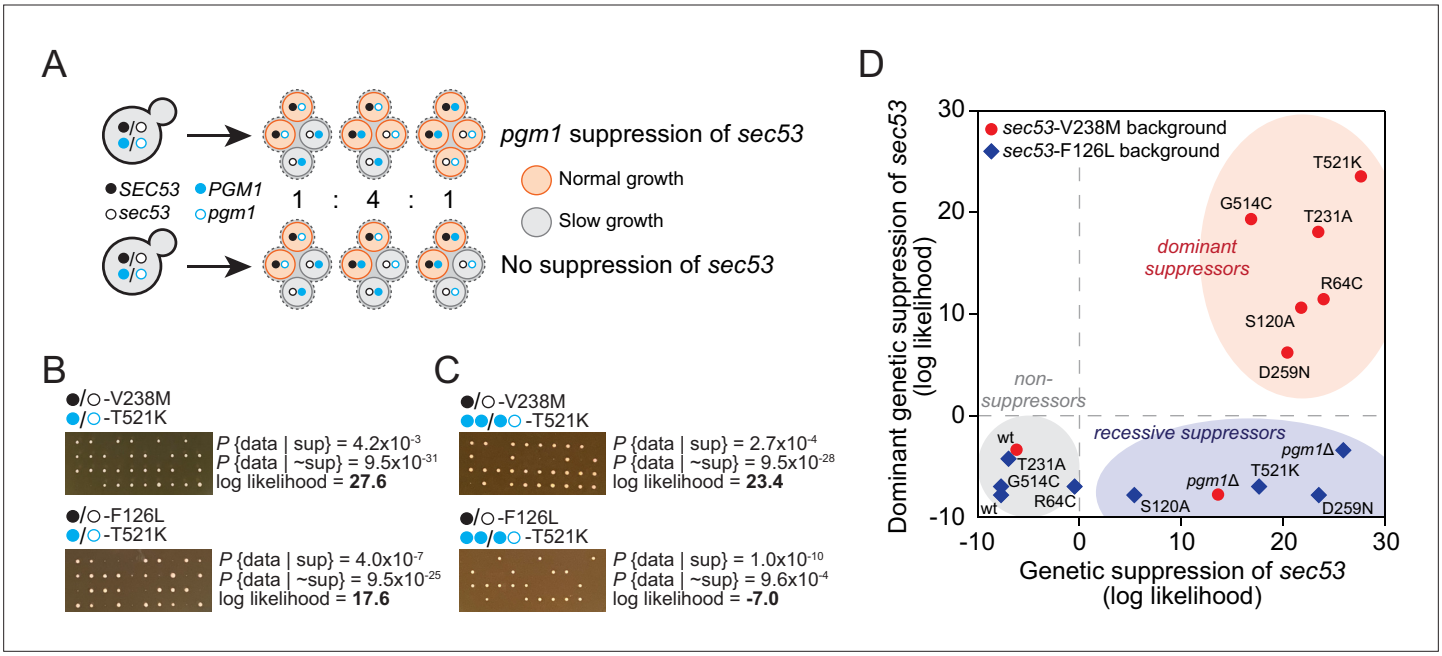

Figure 4. *pgm1* mutations are dominant suppressors of *sec53*-V238M. (**A**) Diagram of possible spore genotypes in the tetrad dissections. Heterozygous (e.g., *SEC53*/*sec53 PGM1*/*pgm1*) diploid strains could produce one of three tetrad genotypes based on allele segregation. (**B**) Example of *pgm1*-T521K dissections in a *sec53*-V238M background (top) and a *sec53*-F126L background (bottom). Listed are the probability and log likelihood of suppression, based on the ratio of normal growth (large colonies) to slow growth (no colonies or small colonies). (**C**) Example of *PGM1*::*pgm1*-T521K dissections in a *sec53*-V238M background (top) and a *sec53*-F126L background (bottom). (**D**) Plot of recessive suppression versus dominant suppression of the *pgm1* mutations in the *sec53*-V238M background (red circles) and *sec53*-F126L background (blue diamonds), based on the tetrad dissections.

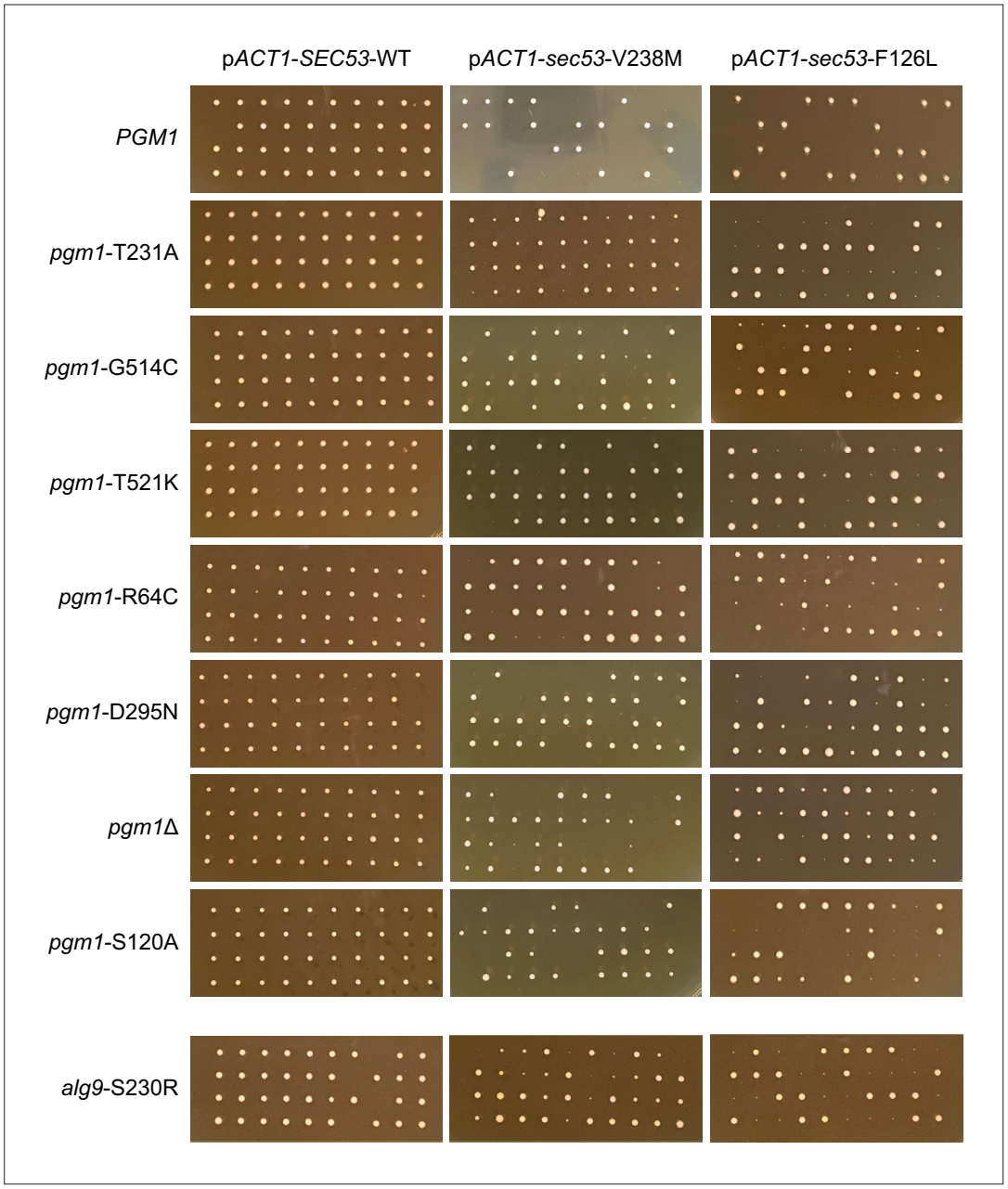

Figure 4—figure supplement 1. Tetrad dissections of *PGM1*/*pgm1* and *ALG9*/*alg9* strains. Ten tetrads were dissected for each strain. Spores from the same tetrad are grouped vertically. The parental diploid strains contained heterozygous *SEC53*/*sec53* alleles and heterozygous *PGM1*/*pgm1* or *ALG9*/*alg9* alleles.

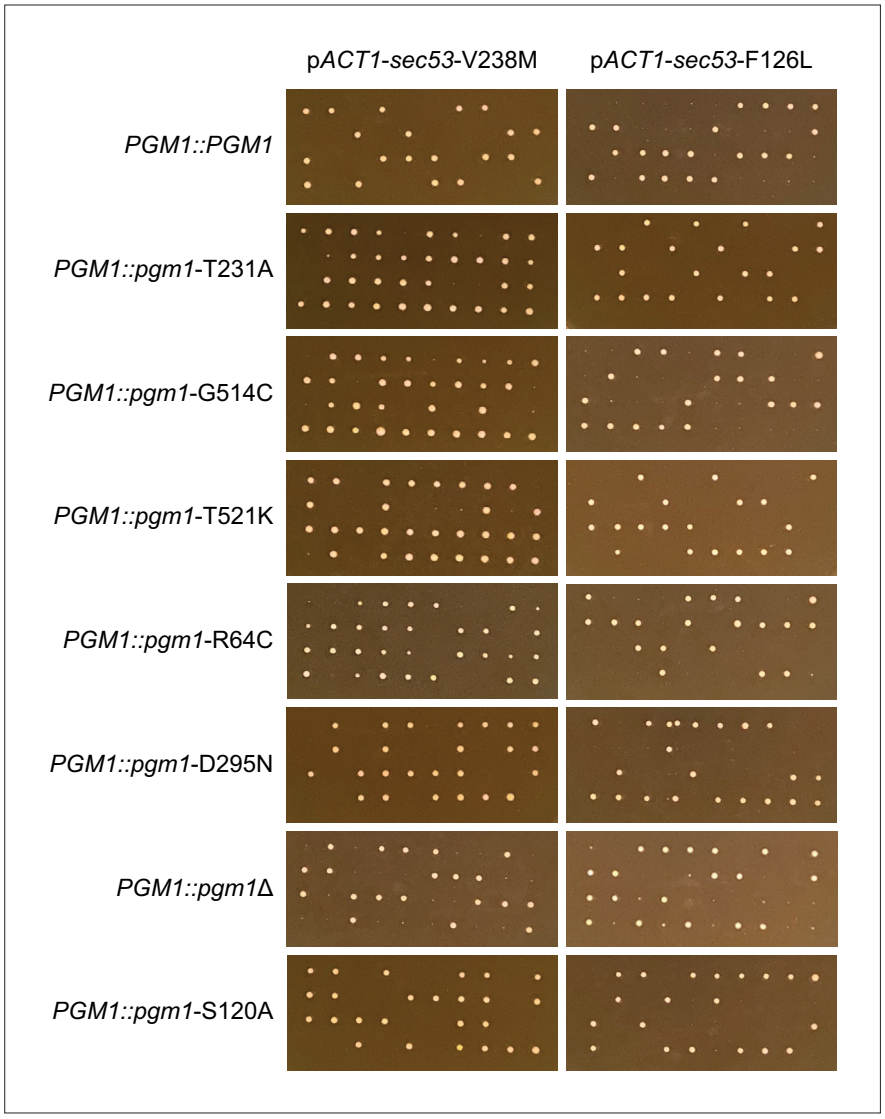

Figure 4—figure supplement 2. Tetrad dissections of *PGM1*-linked strains. Ten tetrads were dissected for each strain. Spores from the same tetrad are grouped vertically. The parental diploid strains contained heterozygous *SEC53*/*sec53* alleles and four copies of *PGM1*; a wild-type copy of *PGM1* was introduced next to the endogenous *PGM1* ORF. Each haploid spore, then, contained either two wild-type copies (*PGM1::PGM1*) or a wild-type and mutant copy (*PGM1::pgm1*).

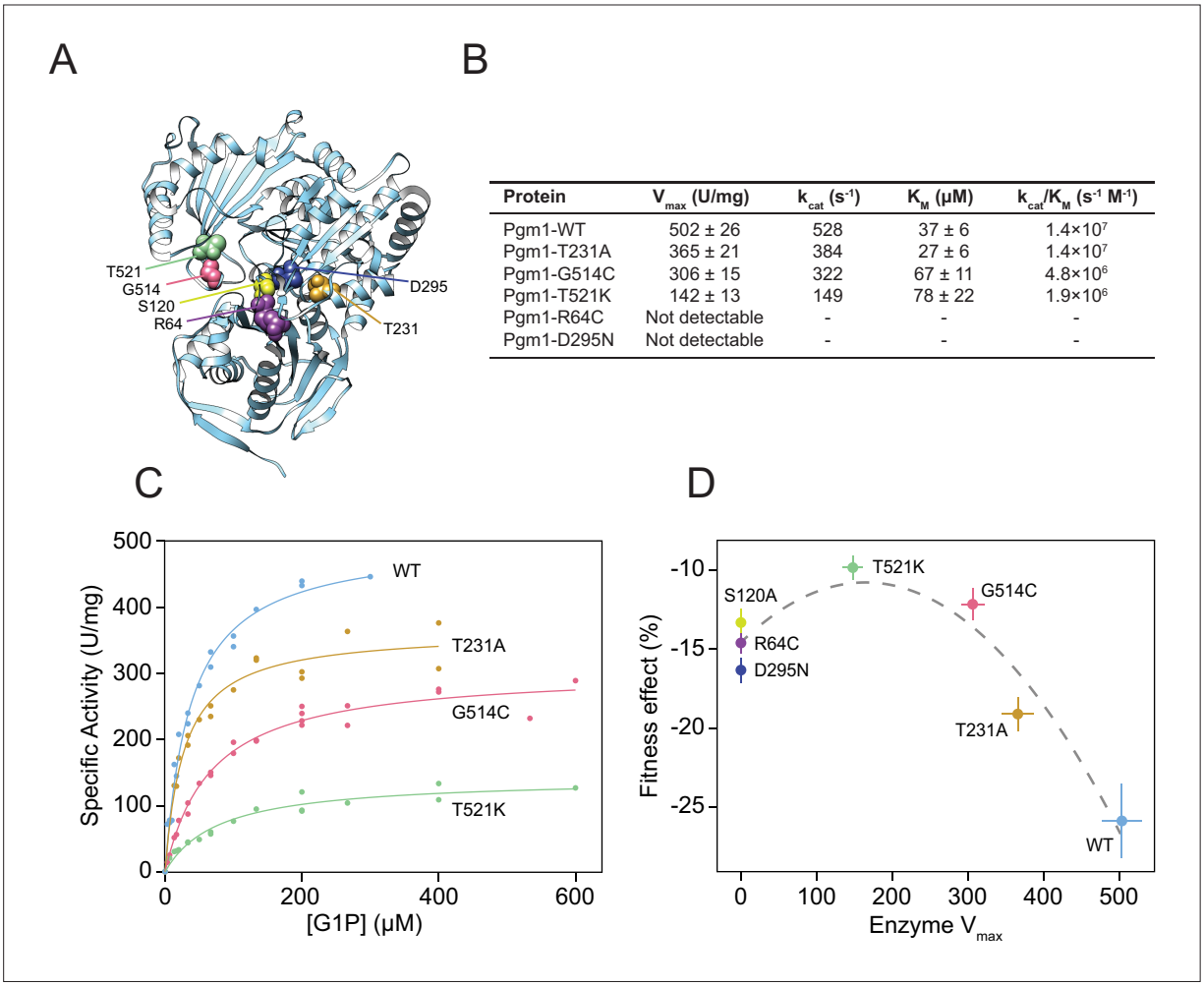

Protein	V_{max} (U/mg)	k_{cat} (s^{-1})	K_M (μM)	k_{cat}/K_M (s^{-1} M^{-1})
Pgm1-WT	502 ± 26	528	37 ± 6	1.4×10^{7}
Pgm1-T231A	365 ± 21	384	27 ± 6	1.4×10^{7}
Pgm1-G514C	306 ± 15	322	67 ± 11	4.8×10^{6}
Pgm1-T521K	142 ± 13	149	78 ± 22	1.9×10^{6}
Pgm1-R64C	Not detectable	-	-	-
Pgm1-D295N	Not detectable	-	-	-

Figure 5. Complete loss of Pgm1 activity overshoots a fitness optimum. (**A**) AlphaFold structure of *S. cerevisiae* Pgm1 (***Jumper et al., 2021***). Mutated residues shown as spheres. (**B**) Kinetic parameters of recombinant Pgm1 enzymes as determined by a coupled enzymatic assay. Values ± 95% confidence intervals. (**C**) Michaelis–Menten curves of wild-type and mutant Pgm1. Replicate measurements are plotted as circles. (**D**) Pgm1 enzyme V_{max} versus the corresponding allele's fitness effect in the diploid p*ACT1-sec53*-V238M background (as shown in ***Figure 3A***). Horizontal and vertical error bars represent 95% confidence intervals. Best fit regression shown as a dashed curve ($y = 14.583 + 0.04613x - 0.00014x^2$, $R^2 = 0.907$, df = 4, $F = 37.34$, p = 0.0258, analysis of variance [ANOVA]). Note that we did not measure Pgm1-S120A activity and assume null activity.

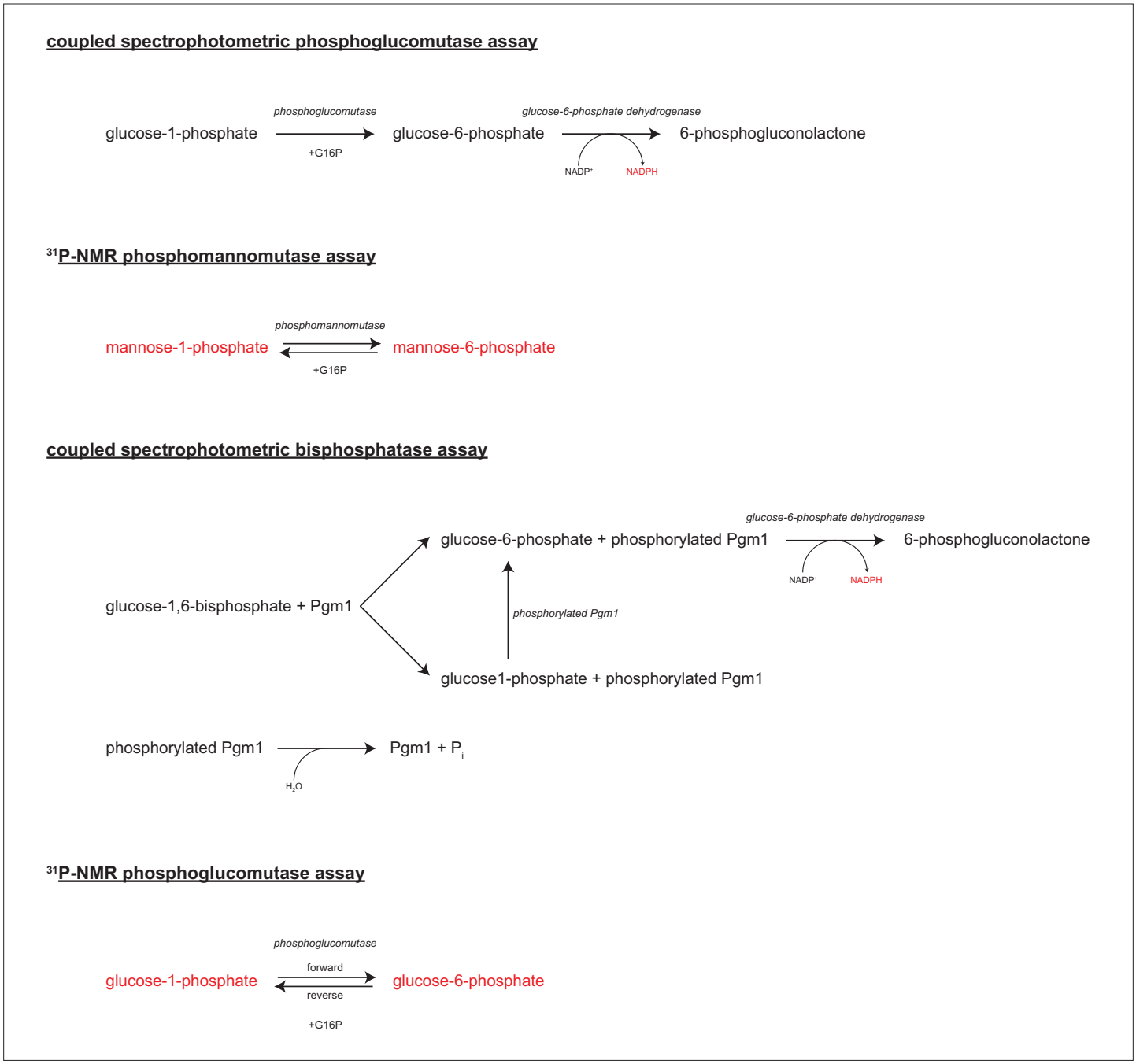

Figure 5—figure supplement 1. Enzymatic assays. Diagrams of the enzymatic reactions assayed in this study.

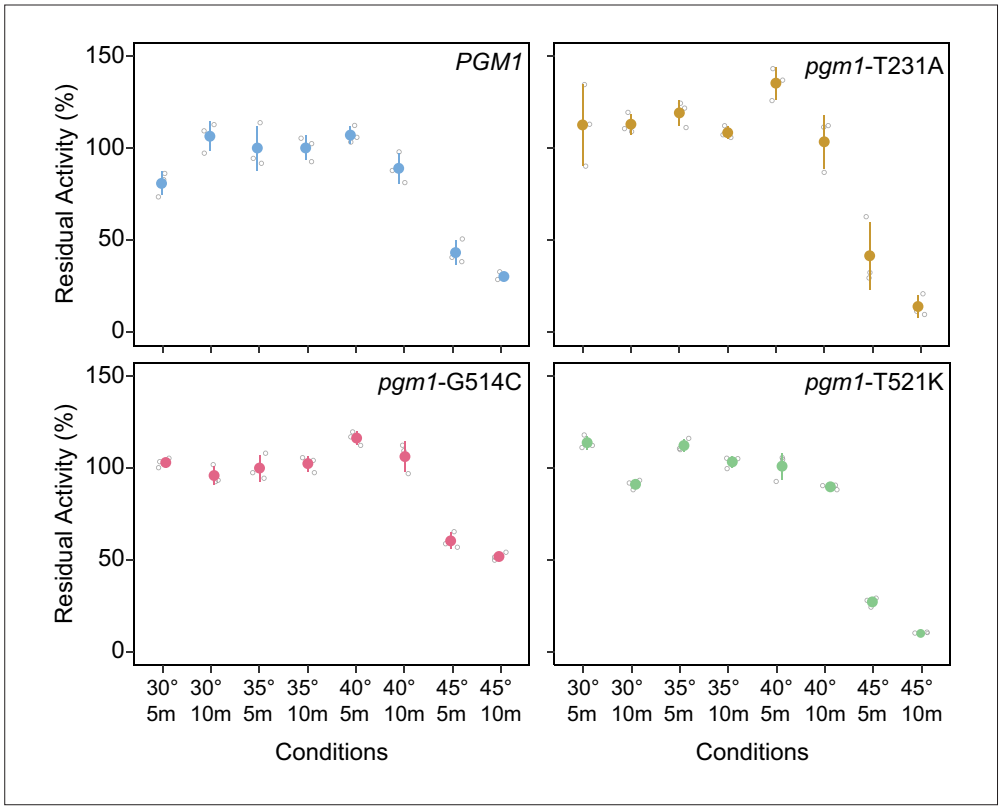

Figure 5—figure supplement 2. Thermostabilities of mutant Pgm1. Average residual activity and standard deviations of recombinant Pgm1 enzymes determined after incubation at the conditions described on the *x*-axis. Replicate measurements plotted as gray circles. Proteins were incubated in the presence bovine serum albumin (BSA; 0.1 mg/ml).

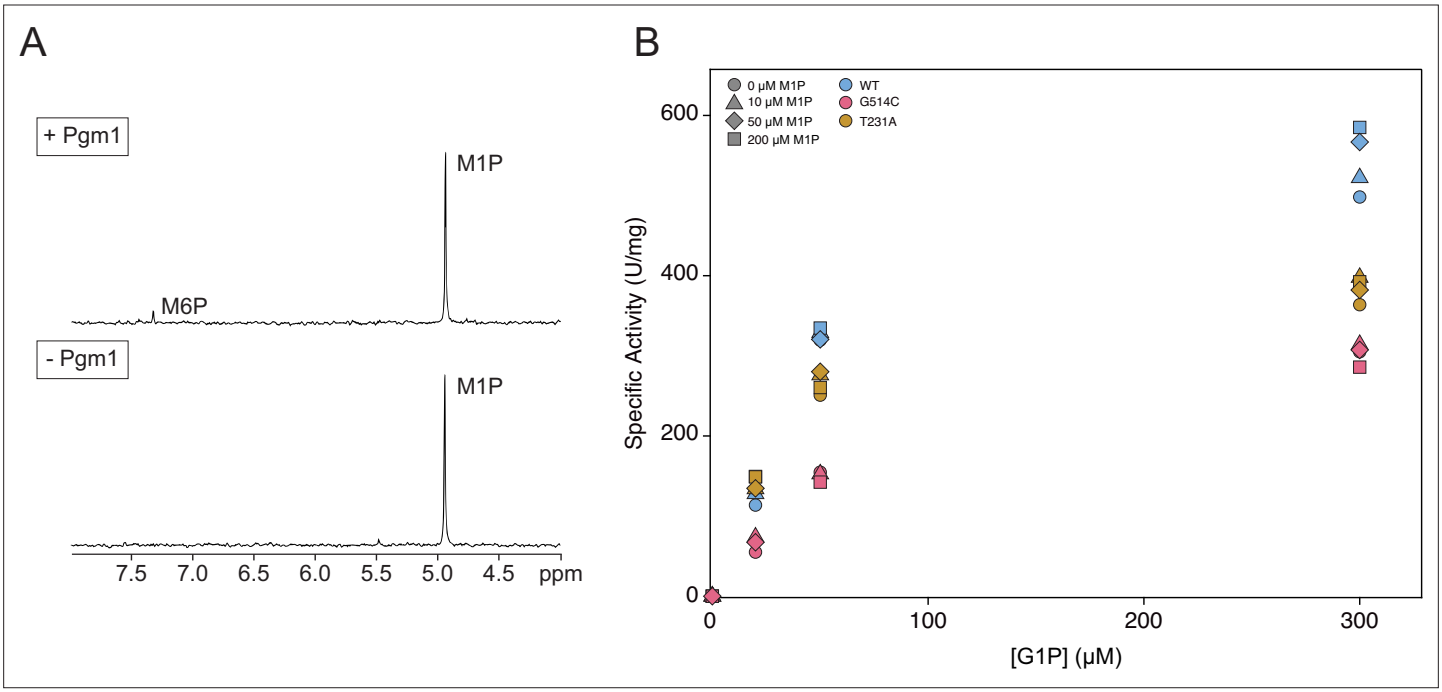

Figure 5—figure supplement 3. Phosphomannomutase activity of mutant Pgm1. (**A**) Representative phosphomannomutase assay by ^{31}P-NMR spectroscopy. Pgm1 was incubated with 1 mM mannose-1-phosphate (M1P) and 20 µM glucose-1,6-bisphosphate (G16P) for 0 or 60 min. The amount of M1P or M6P was measured by integrating the area of the signals and comparing them to creatine phosphate, added as an internal standard. (**B**) Spectrophotometric phosphoglucomutase assays were conducted at different concentrations of glucose-1-phosphate (G1P) and M1P. Shapes indicate varying concentrations of M1P and colors indicate Pgm1 variants.

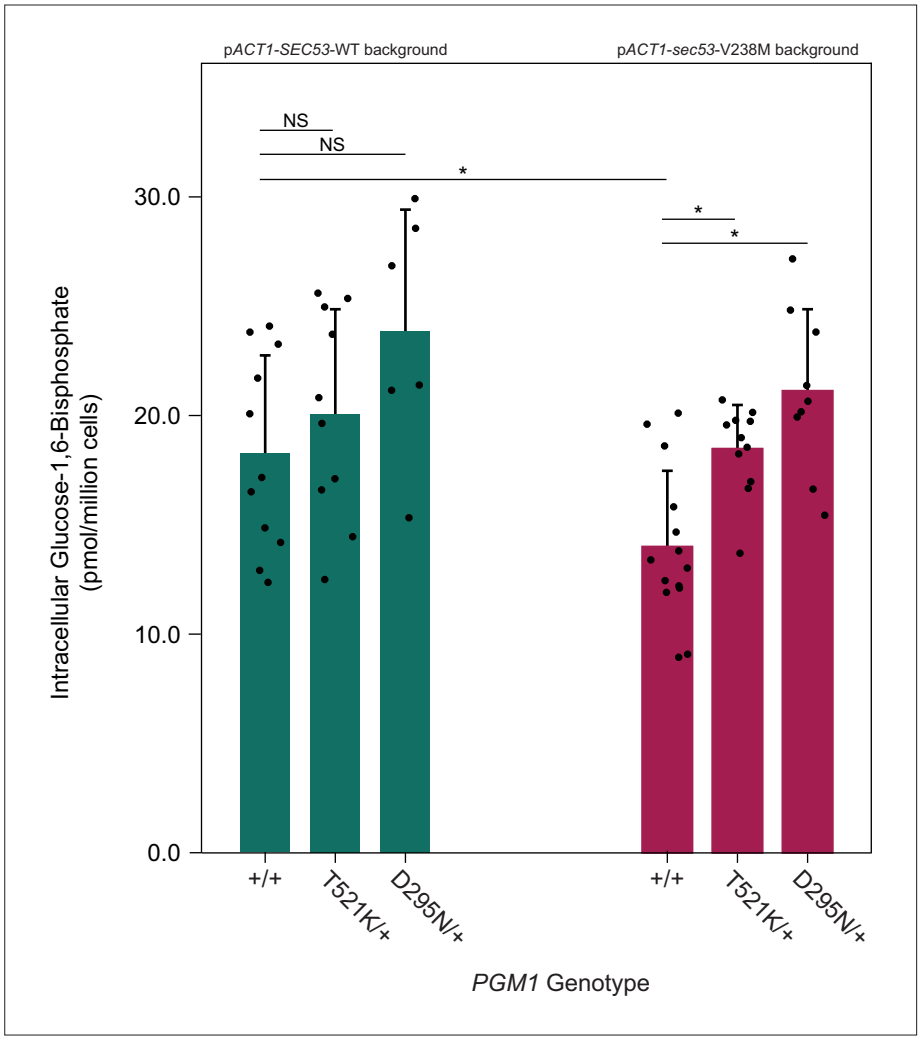

Figure 5—figure supplement 4. *pgm1* mutations increase glucose-1,6-bisphosphate (G16P) levels in the p*ACT1-sec53*-V238M background. Average abundance and standard deviations of G16P in *SEC53*-WT and *sec53*-V238M strains following metabolite extraction. Plus signs (+) indicate wild-type alleles. Replicate measurements plotted as circles. Asterisks (*) represent statistically significant differences (Mann–Whitney *U*-test, $p < 0.01$).

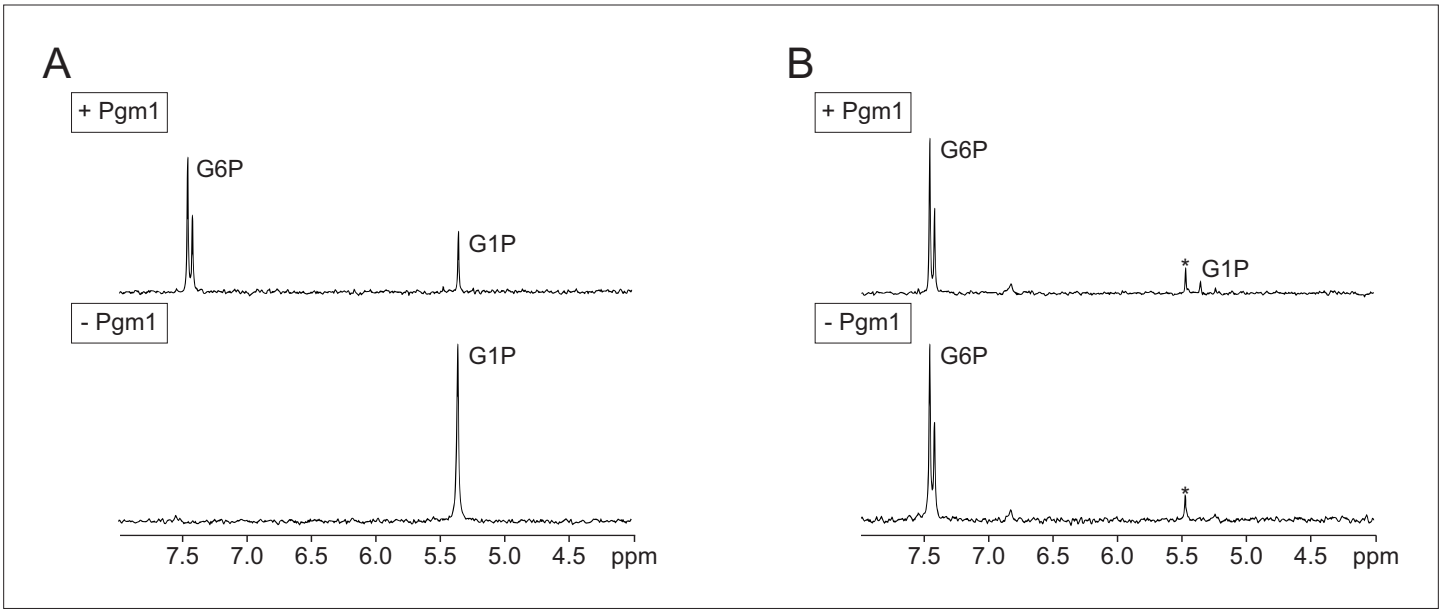

Figure 5—figure supplement 5. Representative forward/reverse phosphoglucomutase assay. Equal amounts of Pgm1 were incubated with glucose-1-phosphate (G1P) (**A**) or G6P (**B**) in the presence of glucose-1,6-bisphosphate (G16P) for 0, 5, 10, or 15 min. The amount of the substrates and products was measured by integrating the area of the signals and comparing them to creatine phosphate, added as an internal standard. Asterisks (*) indicate P_i contaminants.